JTTEE5 18:331–342
DOI: 10.1007/s11666-009-9327-0
1059-9630/$19.00 © ASM International

Influence of Particle Velocity on Adhesion of Cold-Sprayed Splats

S. Guetta, M.H. Berger, F. Borit, V. Guipont, M. Jeandin, M. Boustie, Y. Ichikawa, K. Sakaguchi, and K. Ogawa

(Submitted August 8, 2008; in revised form April 8, 2009)

In cold spray, innovative coating process, powder particles are accelerated by a supersonic gas flow above a certain critical velocity. Particles adhesion onto the substrate is influenced by particle impact velocity, which can change dramatically depending on particle position from the core of the jet. In the present work, an original experimental set-up was designed to discriminate the particles as a function of the levels of velocity to investigate the influence of this parameter on adhesion. Particles at given positions could therefore be observed using scanning electron microscope, which showed different morphologies as a function of impact velocity. High pressure and temperature at the interface during impact were calculated from numerical simulations using ABAQUS®. Transmission electron microscope analyses of thin foils were carried out to investigate into resulting local interface phenomena. These were correlated to particle impact velocity and corresponding adhesion strength which was obtained from LAser Shock Adhesion Test.

Keywords adhesion, cold spray, high-velocity impact, LASAT, numerical simulation, splat

1. Introduction

Cold-sprayed coatings can be achieved only when the velocity of in-flight particles exceeds a certain critical velocity (Ref 1, 2). Therefore, the velocity prior to impinge on the substrate is the most important parameter in cold spray (Ref 3). However, this in-flight velocity is not uniform in the jet flow, particularly when particles go through the shock wave area termed as the ''bow shock'' area (Ref 4). In this area, the smallest particles can be decelerated dramatically or deflected away from the substrate (Ref 5). This work focused therefore on particle impact velocity.

A good coating-substrate adhesion is essential. However, to investigate into coating adhesion and cohesion, the study of adhesion of elementary particles, namely splats, onto the substrate is required.

Even though particle adhesion mechanisms have not been yet elucidated, it can be assumed they are influenced by particle impact velocity, which results from spraying conditions (Ref 6, 7), particle diameter (Ref 8), and particle position from the center of the jet (Ref 9). Different splat morphologies observed by scanning electron microscopy (SEM) as a function of spraying conditions and positions from the center of the particle jet are shown in Fig. 1(a) for particles about 10 μm in diameter and in Fig. 1(b) for particles about 60 μm in diameter.

In the present study, a method to discriminate the particles as a function of velocity was developed to study the influence of impact velocity on adhesion. The latter could be measured from the exploiting of the laser shock phenomenon. Laser shock-based processing could already simulate experimentally cold spray (Ref 10) and could quantify coating adhesion via LASAT (LAser Shock Adhesion Test), as, for the latter, formerly shown at ITSC 2002 (Ref 11). In this study, an original extension of LASAT was developed to be applied to deposited splats.

2. Spraying

2.1 Materials and Cold Spray

CGT Kinetic 3000-M facilities equipped with a ''MOC'' nozzle were used to cold spray. This circular nozzle ''MOC'' (CGT-GmbH) has an inner diameter of 6.6 mm, an expansion ratio of 6.0, and a total length of 175 mm. During sprayings, particles were accelerated using nitrogen (N_2) gas. At a given pressure, e.g. 30 bar (3 MPa) in the present work, particle velocity fairly increases with temperature, e.g. about 10% from 400 to 600 °C typically. Those conditions coupled with a discriminating set-up allowed to select particle impact velocities and possibly temperatures for particles before particle impinging.

S. Guetta, F. Borit, V. Guipont, and **M. Jeandin**, Ecole des Mines de Paris (ENSMP), Competence Centre for Spray Processing (C2P), Evry Cedex, France; **M.H. Berger**, Ecole des Mines de Paris (ENSMP), Centre des Matériaux P.M. Fourt, Evry Cedex, France; **M. Boustie**, Ecole Nationale Supérieure de Mécanique et d'Aérotechnique (ENSMA), Laboratoire de Combustion et Détonique (LCD), Poitiers, France; and **Y. Ichikawa, K. Sakaguchi,** and **K. Ogawa**, Graduate School of Engineering, Fracture and Reliability Research Institute (FRI), Tohoku University, Sendai, Japan. Contact e-mail: serge.guetta@ensmp.fr.

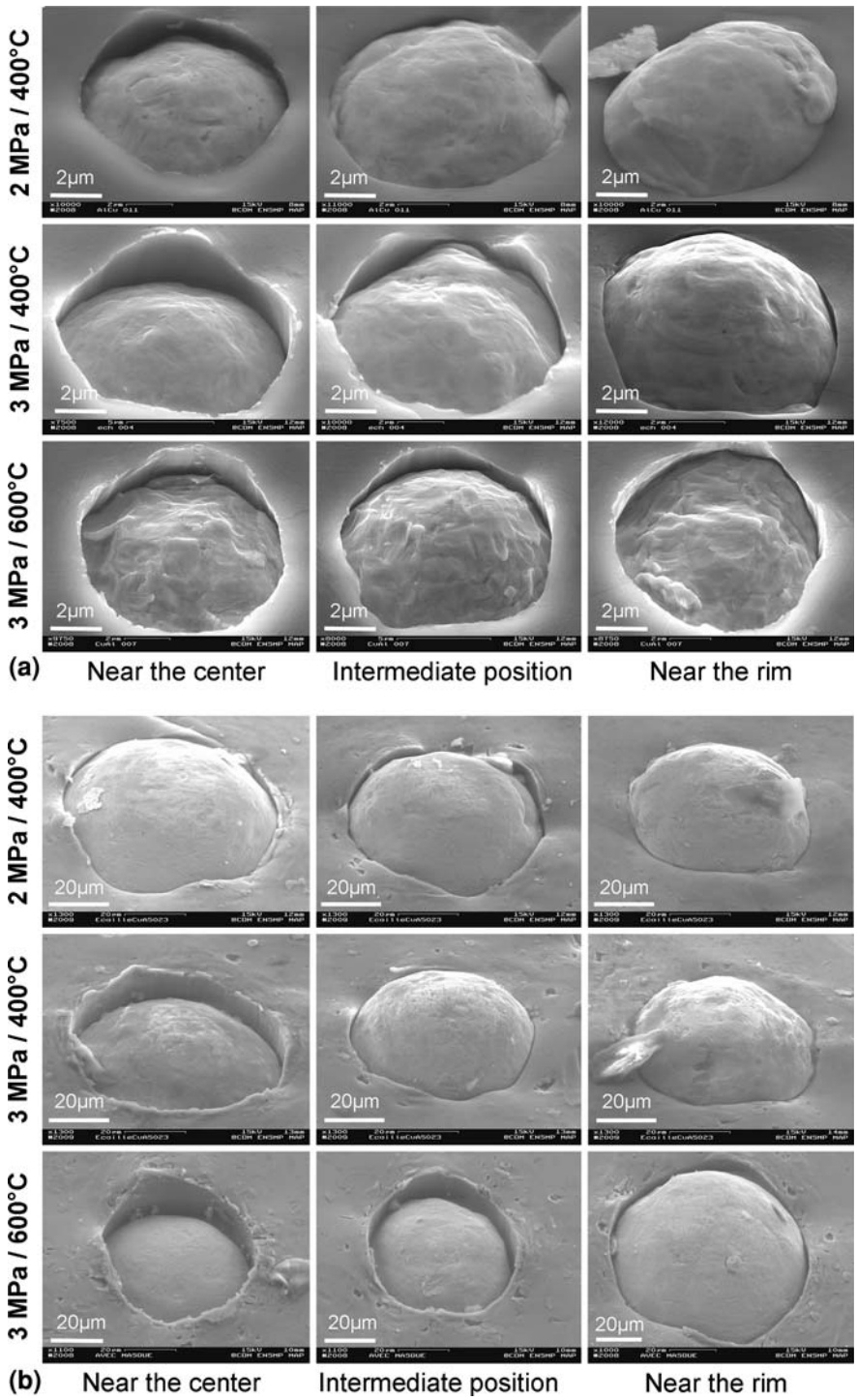

Fig. 1 Different splat morphologies observed by SEM as a function of spraying conditions and positions from the center of the particle jet (a) for particles about 10 μm in diameter and (b) for particles about 60 μm in diameter

This study was carried out with pure aluminum substrate and copper powders within two ranges of particle size: 10 and 60 μm, respectively. This two-material reactive system was kept to result in first layer bonding, which corresponded to the first step to build-up a coating, with physical-chemical interactions at the interface.

2.2 Particle Collecting System

The purpose of this study was to investigate the particle-substrate interface as a function of particle impact velocity. Due to noticeable variations of the velocity between the center and the rim of the jet, i.e. of about 25% (Ref 9),

discriminating particles could not result from a mere passing of the gun above the substrate at a low powder rate, if so, velocity overlapping would occur. Near the center of the sprayed line, particles would come from the center and rim of the jet (Fig. 2).

A sample without velocity overlapping could be obtained by keeping the gun and the substrate stationary. A specific set-up made of a mask was designed (Fig. 3). Only the mask could move horizontally. During this experiment, particles were sprayed onto the mask except when the slit, the gun, and the substrate were aligned.

The standoff distance between the mask and the nozzle exit was chosen as 37 mm. Substrates were positioned 8 mm below the mask. The latter had a traverse speed of 250 mm s^{-1}. This velocity narrowly depended on the powder feed rate, 0.5 rotation per minute, in order to obtain discriminated particles onto the substrate. A rectangular slit was machined (15 mm of length, 1.5 mm of width, and 1 mm of thickness). Nevertheless, some experiments are in process to well understand the influence of the mask on particle impact velocity. Indeed, different sizes and shapes of slit are compared to detect different morphologies for impacted particles.

To facilitate the location of the particles in a cross section, a circular groove was machined before spraying. When knowing that of a particle on the chord, it was easy to determine the corresponding polar coordinates from the center of the jet (Fig. 4).

3. Observation

3.1 Scanning electron microscopy

SEM observation was carried out for several particles of the same diameter approximately but at different positions in the jet, which the corresponding cross sections were obtained by mechanical polishing. This allowed to detect differences in the morphology between particles from the center and from the rim of the jet. Final deformation, particle coverage, material "jettin"' and debonding at the interface highly depended on impact velocity (Fig. 5).

Even though the detection of such a difference was possible as a function of the particle position in the jet, i.e. as a function of particle impact velocity, SEM observation was not enough to understand adhesion mechanisms at the impact. Deformation and temperature modeling was therefore developed to study impact effects. In addition, observation at a lower scale was carried out to exhibit phenomena governing adhesion, using transmission electron microscopy (TEM).

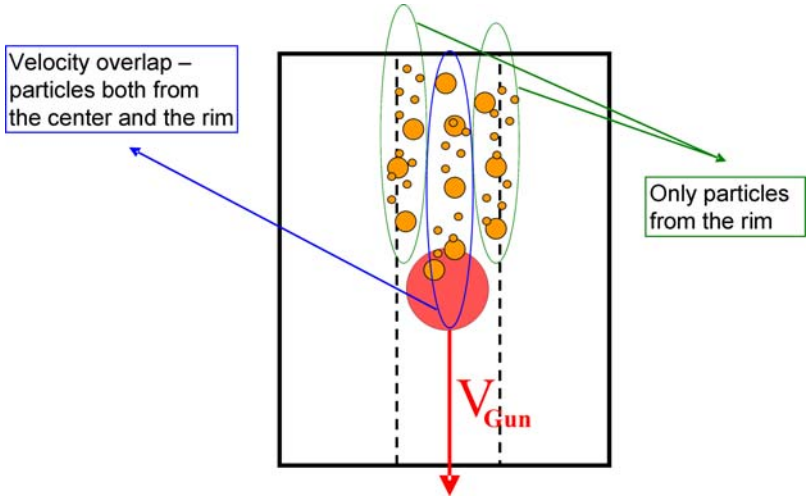

Fig. 2 Schematic illustration of velocity overlapping

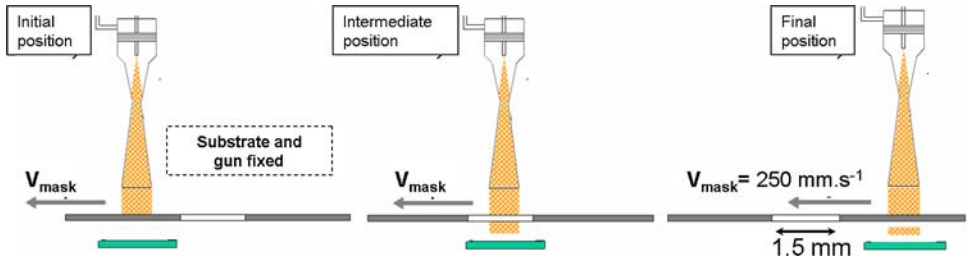

Fig. 3 Sketch of the discriminating set-up

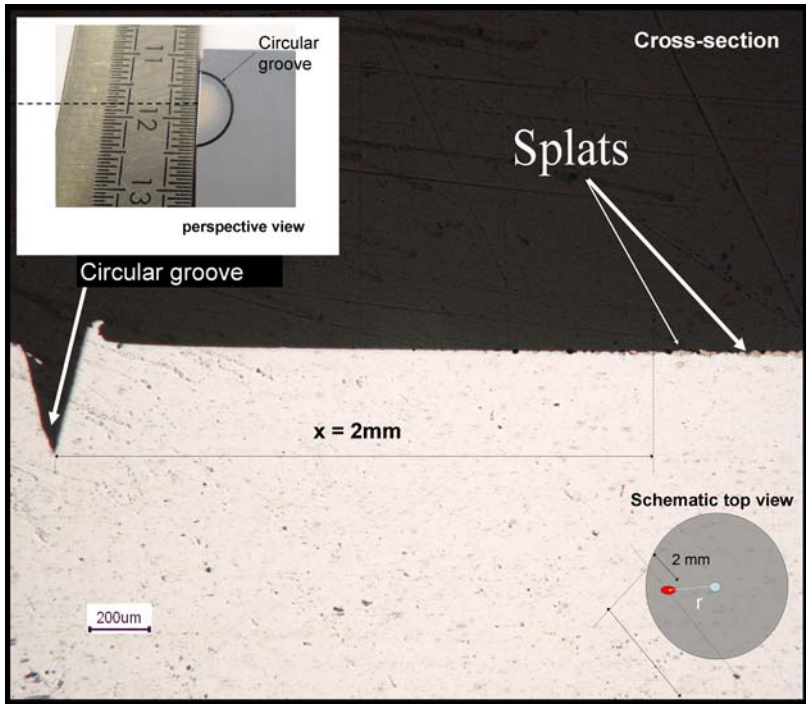

Fig. 4 Cross-sectional view of a sample used in the discriminating set-up (inset: perspective view of a typical sample)

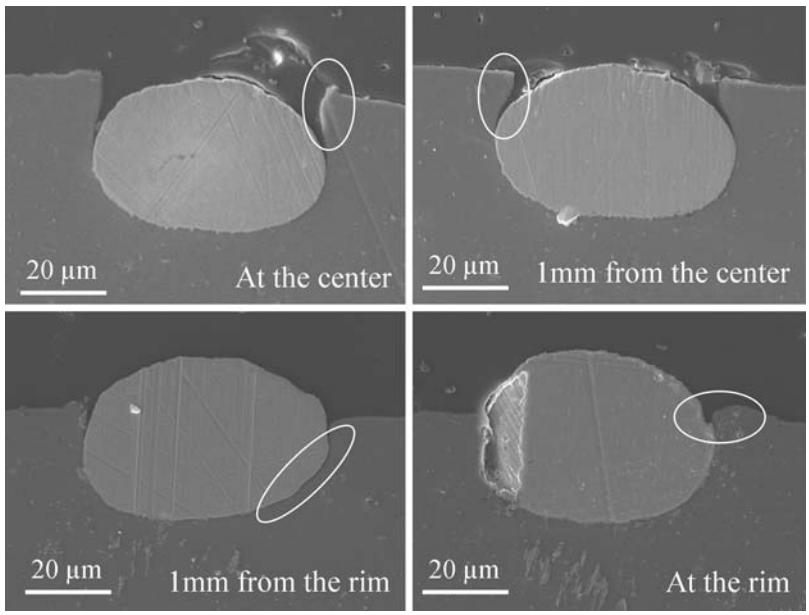

Fig. 5 Different splat morphologies observed by SEM

3.2 Transmission electron microscopy

Physico-chemical mechanisms which occurred during impact had to be studied through TEM of entire splats. Analyses of thin foils obtained from focused ion beam (FIB) processing were carried out to investigate into local interface phenomena. Two copper particles, from the smaller range of particle size (10 µm), sprayed at 30 bar (3 MPa) and 600 °C onto an aluminum substrate, were observed. The first particle was a large particle (20 µm in diameter) located near the rim (Fig. 6a), whereas the second particle was a small particle (10 µm in diameter) located near the center of the jet (Fig. 6b). FIB sections

were observed using a Technai 20ST TEM-STEM equipped with an EADX EDX detector.

In both cases, particles penetrated the substrate deeply, which provoked a material jet. In addition, an aluminum layer could be detected under the tungsten protective layer (used at the FIB stage), at the splat-air interface. Ejected material overlaid the particle as a thin molten film subjected to very high temperature gradients. This quenched film maintained the particle and promoted adhesion. Near the top of the particle, the presence of this amorphous Al-O-based phase and the presence of a preferential gallium ion implantation (used at the FIB stage) in this area indicated either a local transient melting or a large deformation of this amorphous phase in a solid state (Fig. 7).

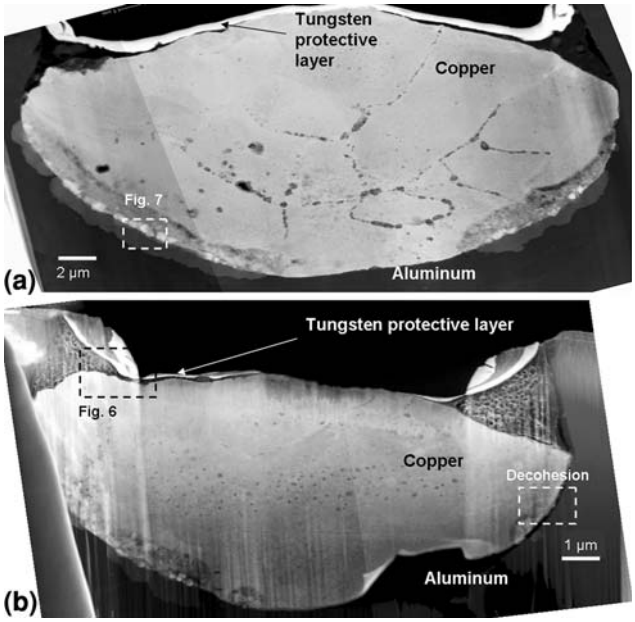

Fig. 6 STEM HAADF pictures of (a) 20 μm and (b) 10 μm copper splats onto aluminum

Moreover, during the impact, grains were highly deformed and shear instabilities could be observed near the interface in both cases. If debonding could occur only for the smallest particle (Fig. 6b), for both particle sizes, large diffusion areas, i.e. above 500 nm of thickness, were observed at the interface. These areas corresponded to those predicted by simulation in which the maximum of temperature was reached (cf. Sect 4.1). In this layer, two nano-crystallized phases were detected and identified as Al_2Cu and Al_4Cu_9 from Fourier transform analysis of high-resolution TEM images and from chemical composition analysis, respectively (Fig. 8a and 9a). Even if the thickness of these reaction-diffusion layers was similar for the two particles, the largest particle presented the widest nano-crystallized area. Near the bottom of the particle, a thick diffusion layer (above 600 nm) could be noticed in both cases (Fig. 9b). Because of highly dynamic conditions during impact, to put forward a conclusion about melting all along the interface was difficult at this stage of the work. A dramatic influence of contact pressure might occur, so that 80 ns was an extremely short interaction time but might be enough to allow a diffusion above several hundreds nanometres, especially near the bottom of the particle.

The optimal size of particles at the highest velocity is claimed to be below 10 μm (Ref 4). The largest particle impinged on the substrate with a lower velocity, all the

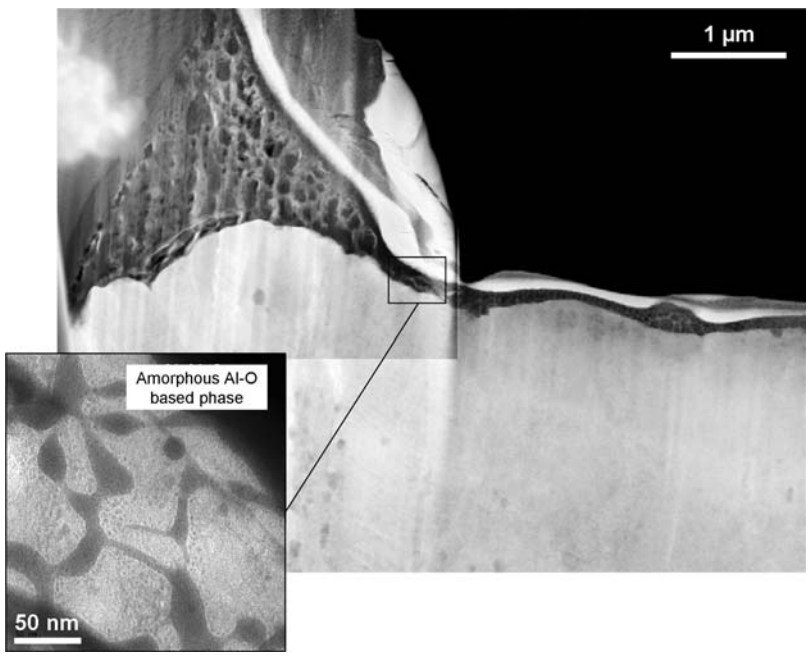

Fig. 7 STEM HAADF view of the amorphous layer (inset: magnified)

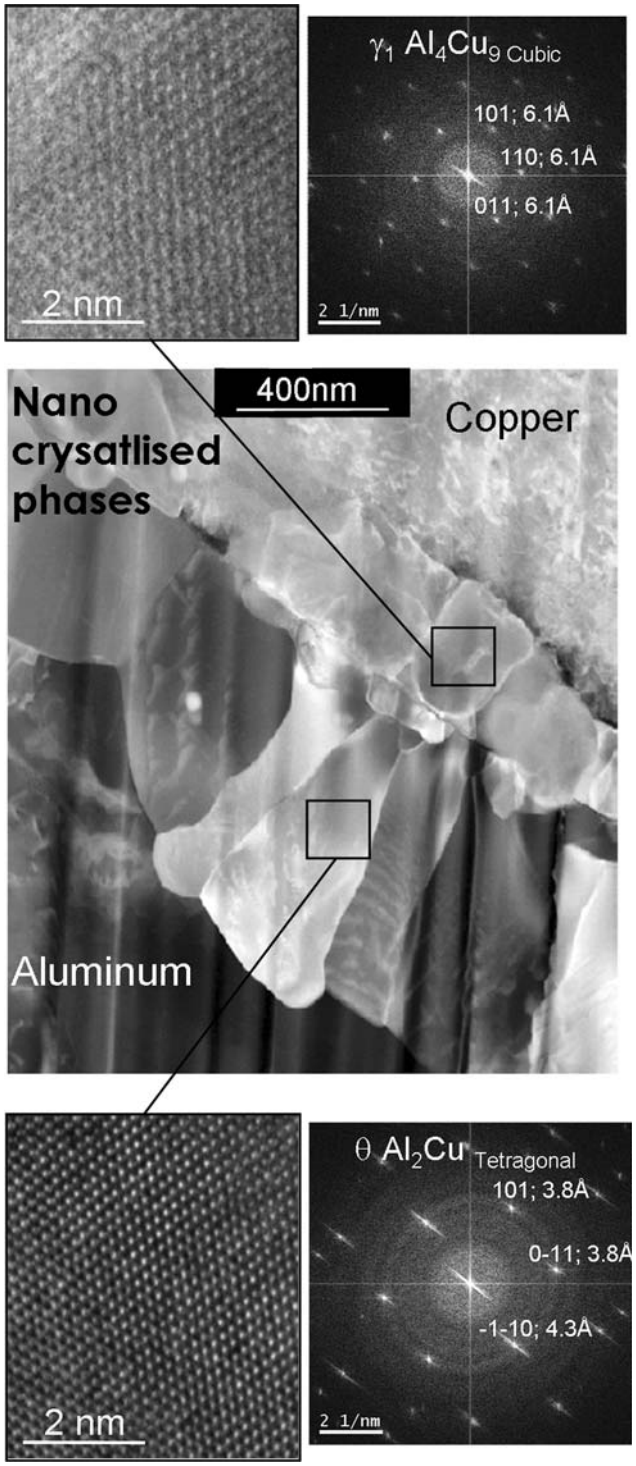

Fig. 8 Microstructure of the splat/substrate interface and Fourier transform analysis of corresponding high-resolution images

more as this particle was located near the rim. Consequently, a better adhesion for the smallest particle could be expected. However, due to the numerous diffusion areas, a higher adhesion might exist for the largest particle. In this case, in contrast to what might be expected, the higher velocity impact would not necessarily correspond to a higher adhesion. An optimum for the impact velocity would therefore result in the best adhesion. For this reason, the development of a suitable adhesion test, i.e. applied to small objects such as splats, was needed.

4. Numerical Simulation

4.1 Particle Impact Modeling

Using numerical simulations, macroscopic parameters such as impact velocity or impact temperature could be related to microscopic parameters such as local temperature, tangential velocity, or contact pressure at the interface. Numerical simulations of particle impact were developed to understand which phenomena occurred during deceleration and to determine very local areas to be observed by TEM. A correlation between microscopic parameters and nanoscale observation could therefore be established.

The two complementary approaches, i.e. simulation and observation, therefore allowed to correlate macroscopic parameters such as impact velocity or impact temperature to nano-scaled phenomena such as melting or nanocrystallization.

Particle deformation at the impact was studied using Abaqus® finite element code in the explicit version 6.5.1 (Ref 12). This two-dimensional axisymmetric analysis was suitable for the studying of strain hardening, thermal softening, heating due to friction and plastic/viscous dissipation.

In this simulation model of particle impact, thermal diffusion through each material was taken into account. However, thermal diffusion through the interface was not considered because adiabatic heating for particle and substrate was assumed (Ref 13). The raise of temperature in materials was mainly due to dissipation into heat of 90% of the stored energy by plastic strain. The ''Johnson-Cook'' plasticity model was used with standard parameters which were taken from Ref 14, 15, then slightly modified: $A = 130$ MPa, $B = 160$ MPa, $C = 0.015$, $n = 0.34$ and $m = 1$ for pure aluminum, and $A = 90$ MPa, $B = 292$ MPa, $C = 0.025$, $n = 0.31$ and $m = 1.09$ for copper. Analyses were performed using axisymmetric models with 4-node elements, adaptive meshing near the contact area which permitted particle-substrate separation after contact.

Two impact conditions were selected to carry out this analysis, i.e. 200 and 430 m s^{-1}. Initial temperatures for the particle (20 μm in diameter) and the substrate were assumed to be 40 and 60 °C, respectively. Using the particle collecting set-up, the substrate was slightly heated by the gas flow till stationary conditions were reached.

The results for high-impact velocity and low-impact velocity were compared to feature involved mechanisms and to determine what would lead to a good adhesion.

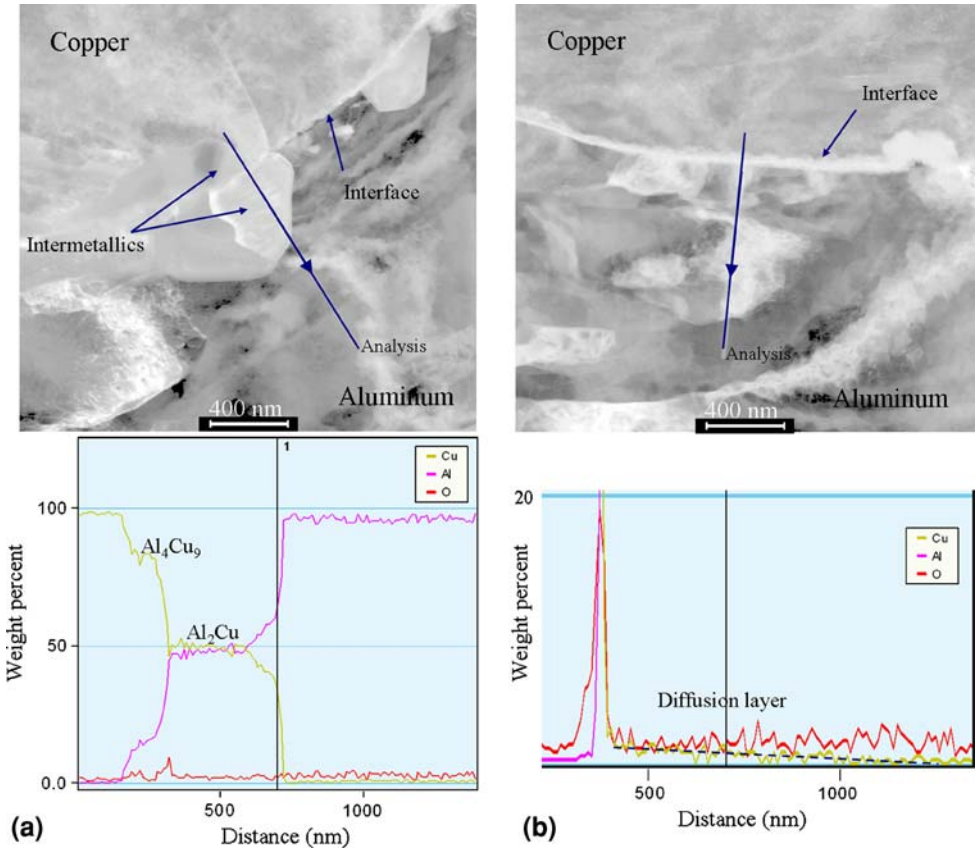

Fig. 9 Chemical composition analysis of (a) nano-crystallized phases and (b) the diffusion layer at the bottom of the particle, measured by EDX along lines depicted on the STEM Dark Field

Local temperature and contact pressure at the interface increased dramatically as a function of velocity impact (Fig. 10). Because diffusion was led by these two parameters, better diffusion for high-velocity impact could be predicted. The highest temperatures were numerically located in a larger area for high-velocity impact, which promoted a larger diffusion. Consequently, a better reaction/diffusion could take place for high-velocity impact, which resulted in a higher adhesion. Moreover, material jettin' and particle overlay from the substrate was observed only for high-velocity impact. This overlaying could hold the particle even though debonding occurred. In simulation, debonding was observed because the simulations were not suitable for describing melting and diffusion.

Therefore, a better mechanical adhesion could be expected for experiments. Consequently, in contrast to low-velocity impact, a high-velocity impact led to large areas of high diffusion which was coupled with high global adhesion.

To corroborate simulations, the calculated final deformation was compared to that observed by TEM actually (Fig. 11). Except for debonding in simulations, as explained above, the final deformation was shown to be fairly the same. Simulations were also compared to nano-scaled TEM observation (cf. Sect 3.2). The highest temperatures were numerically located where the nano-crystallized phases were detected by TEM. Moreover, the calculated temperature near the bottom of the particle was above 150 °C and the contact pressure exceeded 2.5 GPa. Consequently, a large solid-state diffusion could be promoted in this area. This might be correlated to the several hundred nanometres diffusion area detected by TEM. The melting temperature was not reached in simulations even though an amorphous Al-O-based phase was detected by TEM. Therefore, heating by plastic deformation was not high enough to melt aluminum. Other phenomena, not taken into account in the aforementioned model, might promote the rise of temperature at the interface, leading to melting. Consequently, the calculated temperature might be underestimated.

This first validation allowed to use impact simulations as a powerful tool for comparison. However, due to a certain number of rather unknown parameters in Abaqus®, the use of modeling as a quantitative tool could result only from prior calibrating with impact velocity.

Impact simulations consisted of a paramount step before the modeling of LASAT tensile testing. A given

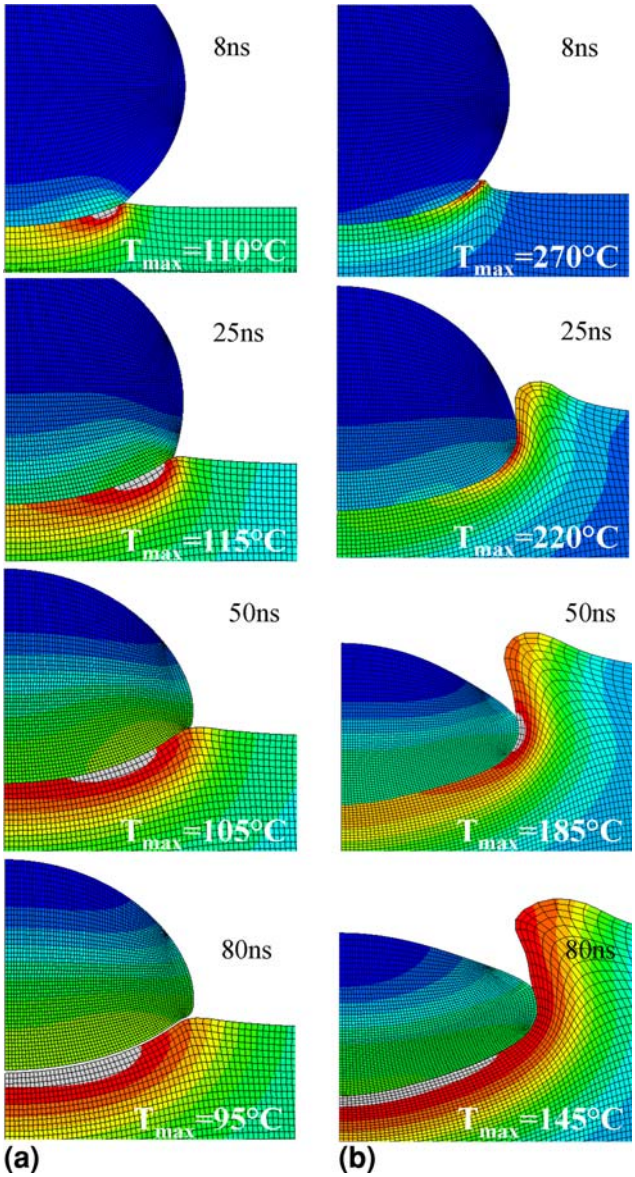

Fig. 10 Temperature of simulated impact for initial velocities of (a) 200 m s^{-1} and (b) 430 m s^{-1}

impact velocity corresponded to a given final deformation. Because tensile testing was sensitive to shapes, it was essential to carry out modeling after impact simulations.

4.2 Tensile Test Modeling

The knowledge of elementary splat adhesion is claimed to be the key point to understand that of the whole coating. If several techniques were available to quantify adhesion of a coating, none of them could be adapted to small objects such as splats, except for LASAT. The latter was therefore developed. Applied to coatings, one-dimensional effects in LASAT resulted in a good understanding of interface adhesion (Ref 11). However, the sole traction generated by the combination of one-dimensional and two-dimensional effects (Ref 15), described in Fig. 12, was high enough to debond splats, as shown by numerical simulations (Fig. 13).

Therefore, particle adhesion level could be determined using a specifically developed set-up. The sample, the top of which surface showed splats, was placed in front of a polymer plane. The upstream laser shock resulted in the debonding of splats, which were collected at the polymer surface (Fig. 14).

For splats, in contrast to the one-dimensional method (Ref 16-18), laser interferometry resulted in measuring the substrate top surface velocity. This was used to calibrate LASATesting numerical simulations before the corresponding traction at interface was calculated.

Because splat debonding highly depended on traction at the interface, the latter was decreased by modifying the laser beam intensity. When the traction was low enough, splats no longer debonded. The level of adhesion was therefore reached.

Consequently, from the coupling of experiments with numerical simulation, the level of adhesion for a class of splats, i.e. for a given velocity, could be determined.

However, the measuring of the level of adhesion for discriminated particles as a function of velocity was of paramount interest to understand the influence of nano-scaled parameters on adhesion. Therefore, using the particle collecting set-up, it was possible to determine the level of traction for every class of particles in the jet. Impact velocity was considered as constant in an area of 500 × 500 μm^2, which defined a given class of splats (Fig. 15).

The aforementioned experimental protocol to debond copper splats with further numerical simulation of the corresponding tensile interfacial stress was applied to particles with 60 μm mean diameter that were cold sprayed on aluminum at 3 MPa and 400 °C. The LASAT was carried with a laser pulse of 25 ns that irradiated a spot area of 4 mm in diameter on the substrate side for three different laser intensities (5.8, 2.2, and 0.5 GW/cm^2, respectively). On the side on which isolated splats were deposited and then laser shocked, the optical observation was carried out near the center of the particle jet that was also aligned with the center of the laser spot. A circular counting area with a 1500 μm diameter was considered to examine the laser shocked zones. In Fig. 16, top views of the as-sprayed areas and corresponding zones after laser shock are given for the three laser intensities. Furthermore, corresponding interfacial tensile stresses calculated in case of a 60 μm particle diameter are also indicated for each laser intensity. It was obvious that copper splats that have underwent the higher selected laser intensity were all debonded and removed from the substrate exhibiting new empty craters. On the reverse, in case of the lowest laser intensity, copper splats were all remaining adherent after LASAT. This observation showed that LASAT could be suitable to determine a sharp adhesion threshold for a given distribution of isolated splats. Moreover, it has been shown that only a proportion of copper splats could be

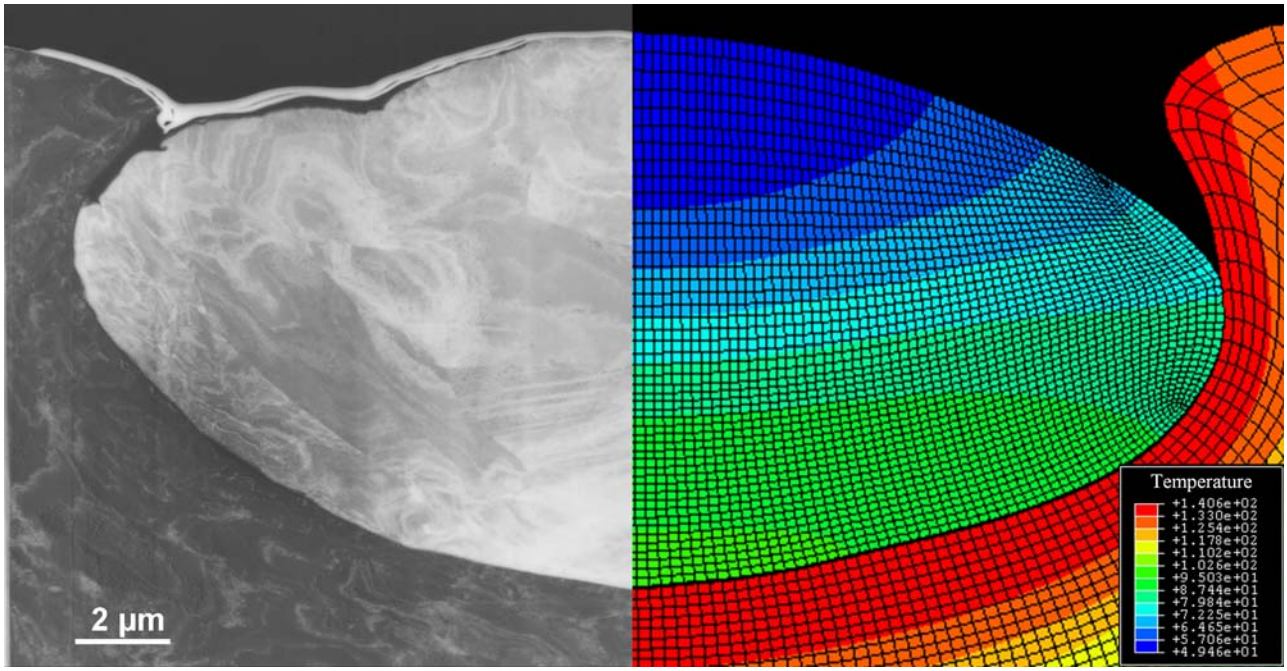

Fig. 11 Final deformation of a copper particle from TEM (left) and calculation (right)

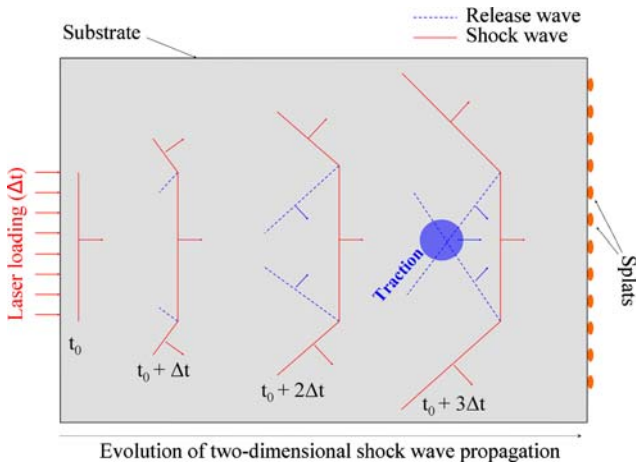

Fig. 12 Schematic illustration of two-dimensional shock wave propagation

debonded when one intermediate laser intensity (2.2 GW/cm^2) was applied. This evidenced that the distribution of splats could exhibit a range of adhesion level depending on individual characteristics like actual particle size and radial position in the jet and corresponding impact velocity. Therefore, further discriminating approach for the LASAT method applied to cold spray splats could be applied to determine the particular adhesion level of each single splat. Experiments are ongoing to assess the influence of splat position from the center of the laser spot on the interfacial tensile stress. Individual level of adhesion would therefore be accurately correlated to impact velocity.

5. Conclusion

The purpose of this study was to investigate the mechanisms of adhesion which could result from cold-sprayed particle impact. Because mechanisms depended on impact velocity, a method to discriminate particles as a function of impact velocity was developed.

TEM observation and numerical simulation showed the mechanical and physico-chemical mechanisms of adhesion which occurred. Mechanical adhesion resulted from both solid material jettin' which kept the particle in the substrate and molten material jettin' which overlaid the particle and improved adhesion. Phyico-chemical adhesion mainly resulted in large diffusion areas located at the interface except near the bottom of the splat. High-contact pressure and high temperature at the interface improved adhesion by promoting diffusion, nano-crystallization and, possibly, local transient melting. A more thorough investigation has to be done to focus on some melting areas at the interface. Moreover, large reaction-diffusion areas which could be observed by TEM were located where numerical simulation predicted high temperature and high contact pressure. Consequently, through TEM observation and simulation, nano-scaled phenomena were correlated to macroscopic parameters such as impact velocity.

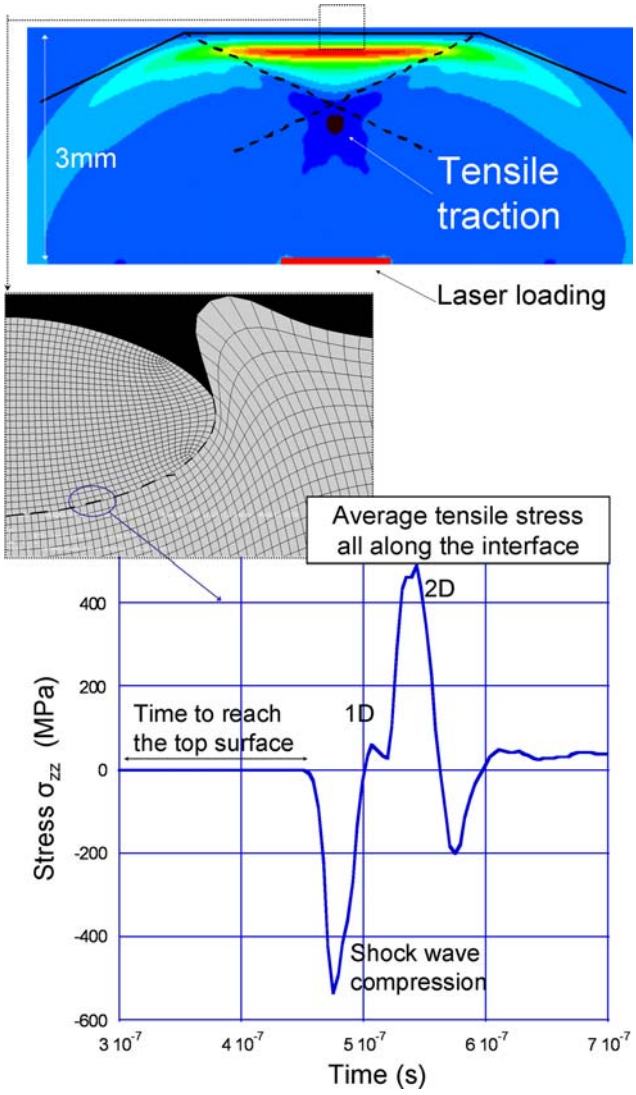

Fig. 13 Two-dimensional LASAT simulation (inset: magnification and calculation of the level of traction generated at the interface)

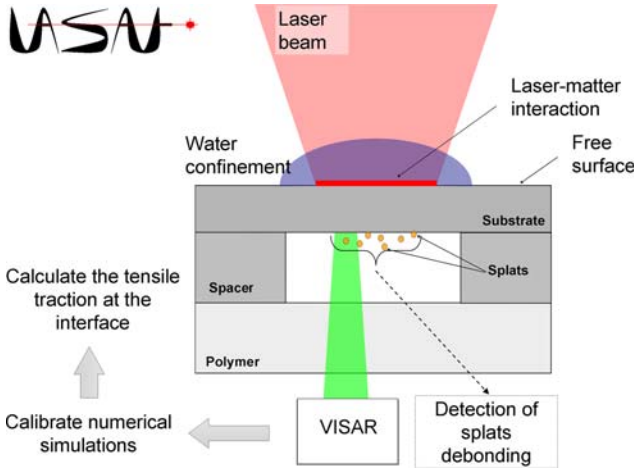

Fig. 14 Schematic illustration of LASATesting set-up for splats

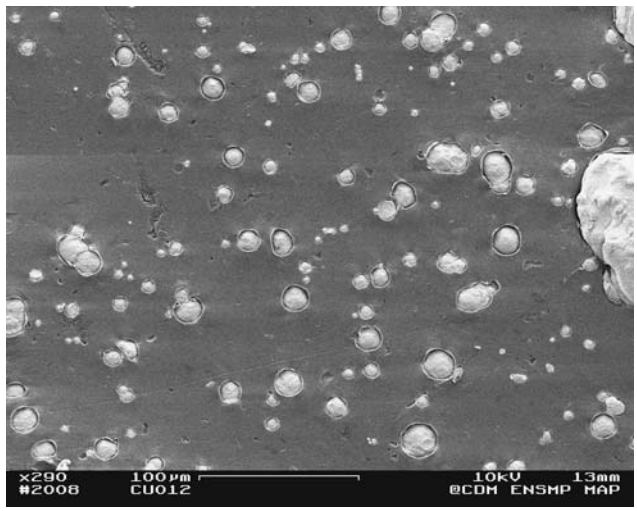

Fig. 15 SEM top view of elementary splats onto an aluminum substrate

Provided they were calibrated from the comparison between calculated and observed final deformation and from measurement of particle impact velocity, numerical simulations would be a powerful tool to determinate quantitatively key parameters such as temperature at the splat-substrate interface. In this study, simulations were validated only from final deformation. This allowed to determine qualitatively which nano-scaled phenomena could occur for different velocities. The measuring of particle impact velocity for every particle, which is currently in process, is carry out as a function of diameter and position in the jet.

The development of an original extension of LASA-Testing resulted in the possibility to debond splats and calculate the corresponding traction at the substrate/splat interface. Consequently, when coupling experiments with numerical simulations, the level of adhesion for a class of splats, i.e. for a given velocity impact, could be determined.

As a whole, this work contributed to a fairly innovative multi-scale approach to cold spray, which claims that splat adhesion is a major intrinsic factor to characterize the process. Splat adhesion can be used as

(i) a calibrating factor prior to actual cold spray,
(ii) a property relevant to coating-substrate interface phenomena, and
(iii) an elementary characteristic to feed micro-to-macro models of overall coating build-up and properties.

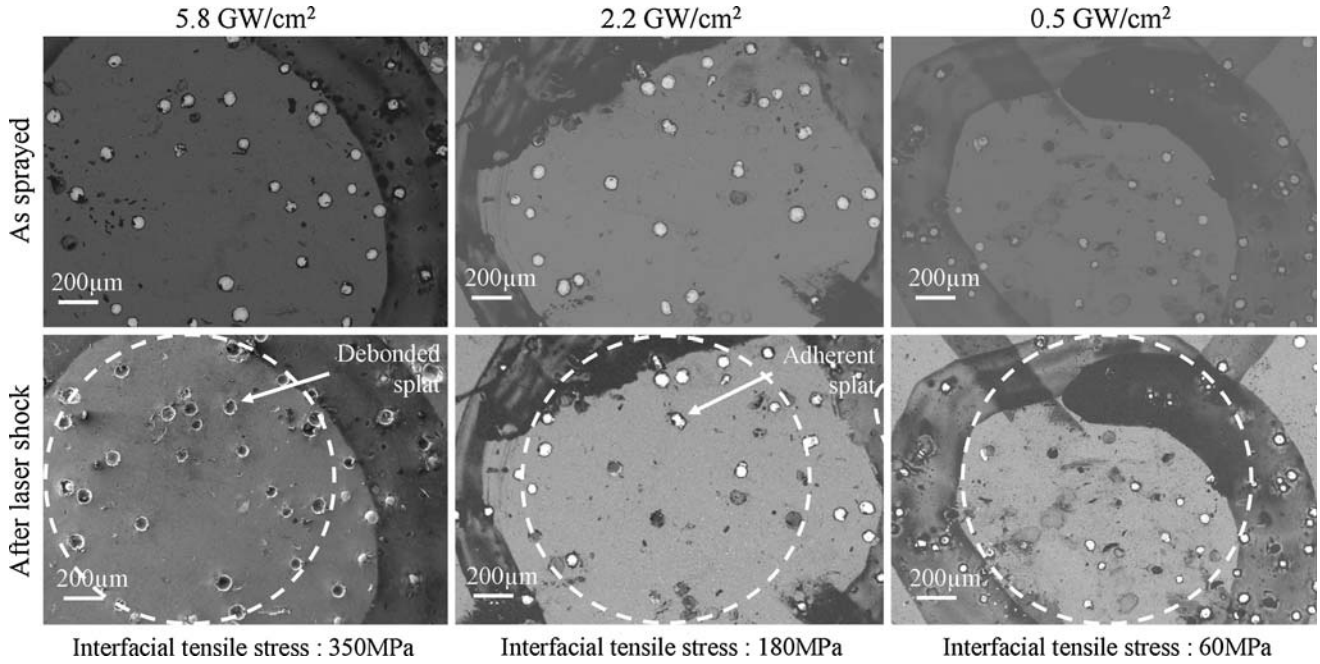

Fig. 16 SEM top views of as-sprayed single splats and after the LASAT test for three different laser intensities and corresponding calculated interfacial tensile stress

Acknowledgments

This work was supported by ADEME ''Agence De l'Environnement et de la Maîtrise de l'Energie'' and EGIDE within a ''Sakura'' program. The authors thank Mr. R. Aron from ADEME for helpful discussion and financial support. Many thanks also to Mr. K. Sakaguchi and Dr. Miyazaki from University of Tohoku–RIFT/ Japan, for help in FIB.

References

1. F. Gartner, T. Stoltenhoff, T. Schmidt, and H. Kreye, The Cold Spray Process and its Potential for Industrial Applications, *J. Therm. Spray Technol.*, 2006, **15**(2), p 223-232 (in English)
2. C.-J. Li, G.-J. Yang, C.-X. Li, H.S. Bang, and W.-Y. Li, Examination of the Estimating Approaches for the Critical Velocity in Cold Spraying, *Proceedings of the International Thermal Spray Conference*, May 14-16, 2007 (Beijing, China), DVS Deutscher Verband für Schweißen, 2007, 123, p 128-134
3. F. Raletz, M. Vardelle, and G. Ezo'o, Critical Particle Velocity Under Cold Spray Conditions, *Surf. Coat. Technol.*, 2006, **201**, p 1942-1947 (in English)
4. J. Pattison, S. Celotto, A. Khan, and W. O'Neill, Standoff Distance and Bow Shock Phenomena in the Cold Spray Process, *Surf. Coat. Technol.*, 2008, **202**(8), p 1443-1454 (in English)
5. C. Donaldson and R.S. Snedeker, A Study of Free Jet Impingement, *J. Fluid Mech.*, 1971, **45**, p 281-319 (in English)
6. M.F. Smith, J.E. Brockmann, R.C. Dykhuizen, D.L. Gilmore, R.A. Neiser, and T.J. Roemer, Cold Spray Direct Fabrication–High Rate Solid State, Material Consolidation, *Materials Research Society Symposium Proceedings*, 1999, 542, p 65-76 (in English)
7. J. Voyer, T. Stoltenhoff, and H. Kreye, Development of Cold Gas Sprayed Coatings, *Thermal Spray 2003: Advancing the Science and Applying the Technology*, B.R. Marple and C. Moreau, Ed., May 5-8, 2003 (Orlando, FL), ASM International, 2003, p 71-78
8. R.C. Dykhuizen and R.A. Neiser, Optimising of the Cold Spray Process, *Thermal Spray 2003: Advancing the Science and Applying the Technology*, B.R. Marple and C. Moreau, Ed., May 5-8, 2003 (Orlando, FL), ASM International, 2003, p 19-26
9. J. Wu, H. Fang, S. Yoon, H. Kim, and C. Lee, Measurement of Particle Velocity and Characterization of Deposition in Aluminum Alloy Kinetic Spraying Process, *Appl. Surf. Sci.*, 2005, **252**(5), p 1368-1377 (in English)
10. S. Barradas, R. Molins, V. Guipont, M. Jeandin, M. Arrigoni, M. Boustie, C. Bolis, L. Berthe, and M. Ducos, Laser Shock Flier Impact Simulation of Particle-Substrate Interactions in Cold Spray, *J. Therm. Spray Technol.*, 2007, **16**(4), p 463-602, 548-556 (in English)
11. S. Barradas, F. Borit, V. Guipont, M. Jeandin, C. Bolis, M. Boustie, and L. Berthe, Laser Shock Flier Impact Simulation of Particle-Substrate Interactions in Cold Spray, *International Thermal Spray Conference*, E. Lugscheider and C.C. Berndt, Ed., March 4-6, 2002 (Essen, Germany), DVS Deutscher Verband für Schweißen, 2002, p 592-597
12. ABAQUS 6.5-1. User manual. Hibbitt, Karlsson & Soerensen. Pawtucket (RI), 2005
13. H. Assadi, F. Gärtner, T. Stoltenhoff, and H. Kreye, Bonding Mechanism in Cold Gas Spraying, *Acta Mater.*, 2003, **51**(13), p 4379-4394 (in English)
14. G.R. Johnson and W.H. Cook, Fracture Characteristics of Three Metals Subjected to Various Strains, Strain Rates, Temperatures and Pressures, *Prog. Astronaut. Aeronaut.*, 1993, **155**, p 165-197 (in English)
15. M. Boustie, J.P. Cuq-Lelandais, C. Bolis, L. Berthe, S. Barradas, M. Arrigoni, T. de Resseguier, and M. Jeandin, Study of Damage Phenomena Induced by Edge Effects into Materials Under Laser Driven Shocks, *J. Phys. Appl. Phys.*, 2007, **40**, p 7103-7108 (in English)
16. M. Boustie, E. Auroux, and J.P. Romain, Application of the Laser Spallation Technique to the Measurement of the Adhesion

Strength of Tungsten Carbide Coatings on Superalloy Substrates, *Eur. Phys. J. Appl. Phys.*, 2000, **12**(1), p 47-53 (in English)
17. S. Barradas, R. Molins, M. Jeandin, M. Arrigoni, M. Boustie, C. Bolis, L. Berthe, and M. Ducos, Application of Laser Shock Adhesion Testing to the Study of the Interlamellar Strength and Coating–Substrate Adhesion in Cold-Sprayed Copper Coating of Aluminum, *Surf. Coat. Technol.*, 2005, **197**(1), p 18-27 (in English)
18. C. Bolis, L. Berthe, M. Boustie et al., *Proceedings of the Conference of the American Physical Society Topical Group on Shock Compression of Condensed Matter*, M.D. Furnish, Y.M. Gupta, and J.W. Forbes, Ed., July 20-25, 2003 (Portland, OR, USA), p 1373-1376